Arch. Metall. Mater. **64** (2019), 1, 79-86

DOI: 10.24425/amm.2019.126221

M. RYWOTYCKI*#, Z. MALINOWSKI*, K. SOŁEK*, J. FALKUS*, K. MIŁKOWSKA-PISZCZEK*

DETERMINATION OF HEAT FLUX AT A SOLID-SOLID INTREFACE

Determining the boundary conditions of heat transfer in steel manufacturing is a very important issue. The heat transfer effect during contact of two solid bodies occurs in the continuous casting steel process. The temperature fields of solids taking part in heat transfer are described by the Fourier equation. The boundary conditions of heat transfer must be determined to get an accurate solution to the heat conduction equation. The heat flux between the tool and the object processed depends mainly on temperature, pressure and time.

It is very difficult and complicated to accomplish direct identification and determination of the boundary conditions in this process. The solution to this problem may be the construction of a process model, performing measurements at a test stand, and using numerical methods. The proposed model must be verified on the basis of parameters which can easily be measured in industrial processes. One of them is temperature, which may be used in inverse methods to determine the heat transfer coefficient.

This work presents the methodology for determining the heat flux between two solid bodies staying in contact. It consists of two stages – the experiment and the numerical computation. The problem was solved by using the finite element method (FEM) and a numerical program developed at AGH University of Science and Technology in Krakow.

The findings of the conducted research are relationships describing the value of the heat flux versus the contact time and surface temperature.

Keywords: continuous casting of steel, heat transfer, inverse method, rolls.

1. Introduction

Heat transfer at the contact of two solid faces is a common effect in processes related to the metallurgical industry. Among others we can find it in the continuous steel casting process – the contact of rolls with the strand face.

The strand cooling process is accompanied by multiple processes, which influence the final product quality [1,2]. Heat transfer during contact of the strand with the cooled withdrawal and support rolls, which are located in the secondary cooling zone, is difficult to describe [3]. The contact area is small when compared to the strand surface area. In the few papers from authors investigating this problem, determination of the heat transfer surface area is approached in a simplified manner. It can be done by providing a share of the contact area at about 0.05 [4] or defining the length of the strand and roll contact arc of about 5 mm [5]. In this case, heat transfer does not have a significant impact on the cooling of the strand withdrawn, however it causes local changes in the surface temperature, which affect the thermal balance of the whole system. The contact pressures are much lower than for hot rolling processes. The contact time is short, however the surface temperature is very high, especially in the first sections of the secondary cooling zone, therefore the heat transfer is intensive. As a result of the impact of rolls on the strand face, local temperature drops of about 100°C [4] are observed, which shows the influence of this heat transfer mechanism on the strand surface temperature (Fig. 1)

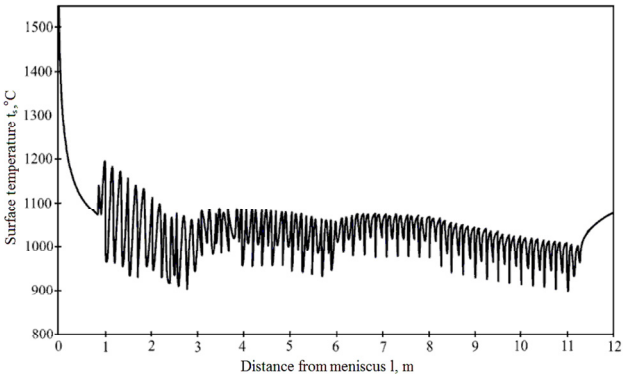

Fig. 1. Changes in the strand surface temperature [6]

The heat transfer at the contact of the rolls with the strand in the continuous steel casting process is rarely discussed in available literature. Most models described concern the value of the heat transfer coefficient. As there are no good models describing this effect, models describing the heat transfer at other processes are adopted. Assuming the heat transfer coefficient

* AGH UNIVERSITY OF SCIENCE AND TECHNOLOGY, FACULTY OF METALS ENGINEERING AND INDUSTRIAL COMPUTER SCIENCE, AL. A. MICKIEWICZA 30, 30-059 KRAKÓW, POLAND

Corresponding author: rywotyc@agh.edu.pl

values that were determined for the rolling process or other heat transfer processes [7-9], which do not correspond to the process nature and are too high, may lead to incorrect determination of the temperature field of the solidifying strand. In publications concerning the subject of heat transfer in the secondary cooling zone, the heat transfer between the strand and rolls is usually neglected or a constant average heat transfer coefficient is assumed within the range 800-2500 W/m^2 K [5,7] or in the form of heat flux defined by the empirical formula [10]:

$$q_s = 11513.7 \cdot t_s^{0.76} \cdot v_{odl}^{-0.2} \cdot \alpha^{-0.16} \quad (1)$$

where: t_s – strand surface temperature, °C; v_{odl} – casting speed, m/min; α – angle of arc of contact between the rolls and the strand, °.

In the study [11], tests and numerical calculations were performed, allowing the value of the heat transfer coefficient and the heat flux absorbed by rolls to be determined. The authors of the paper state that the value of the heat transfer coefficient is not constant for all rolls and its maximum is 2500 W/m^2 K. Also, the amount of heat discharged through the rolls along a length of one metre was evaluated, and it was 24 800 W/m.

2. Methodology for determining the heat flux

This study presents the methodology for determining the heat flux and the heat transfer coefficient between two solid bodies staying in contact. It consists of two stages – the experiment and the numerical computation. The former involves measurements of temperature changes at specific points of the two samples in contact. The latter uses the inverse solution and the finite element method to calculate the heat flux at the contact face. The problem was solved by using the finite element method (FEM) and a numerical program developed at the Department of Thermal Engineering and Environment Protection of AGH University of Science and Technology in Krakow. The schematic diagram of the experimental stand is shown in Fig. 2. In the experiments two samples were used: the Hot sample, which was heated within the furnace, and the Cold sample, which was kept outside the furnace at room temperature. When the Hot sample reached the desired temperature, the furnace was opened and the sample was brought into contact with the Cold one at a constant pressure. The material of the Cold sample was steel WNL (EN steel number 1.2713). The Hot sample was made of steel C45 (EN steel number 1.0503) and was insulated with ceramic fibre. The Hot sample was heated to an initial temperature of 1000°C, 1100°C and 1200°C. The samples were brought into contact under a pressure of 10 MPa. The time of contact was 30 s in each test. At each sample three (COLD) or two (HOT) thermocouples with a diameter of 0,5 mm were installed. For the first sample they were marked as T_{C1}, T_{C2}, T_{C3} and for second one T_{H1}, T_{H2}. During the approach of samples and throughout the test, the output of five thermocouples was monitored and recorded using a computer-based data acquisition system with a frequency of 10 Hz. The full description of the test stand and the experiment is available in the literature [12]. The selection of the test parameters is shown in Table 1.

TABLE 1

Test parameters

Test symbol	Initial temperature for Hot sample t_0 [°C]	Initial temperature for Cold sample t_0 [°C]
1000	1001.20	30.58
1100	1109.86	35.87
1200	1204.65	33.53

The results of the temperature measurements are shown in Fig. 3. The calculation results of that are presented in Fig. 4 allow determining changes in heat fluxes transferred between the samples at various temperature. Numerical calculations were

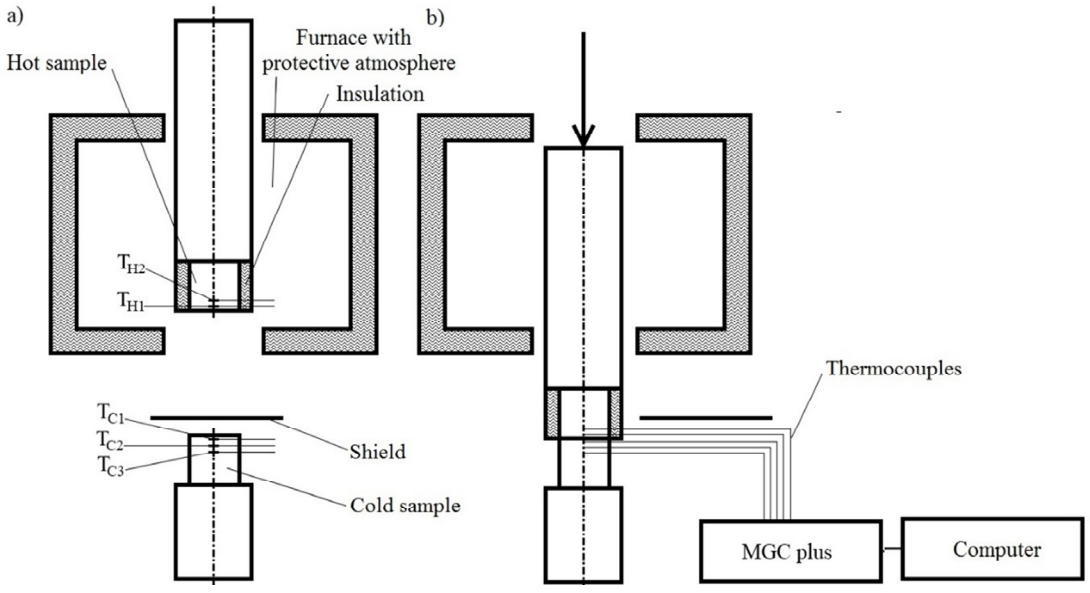

Fig. 2. Schematic diagram of the experiment: a) The heating of a sample in the furnace; b) The positions of samples during the test

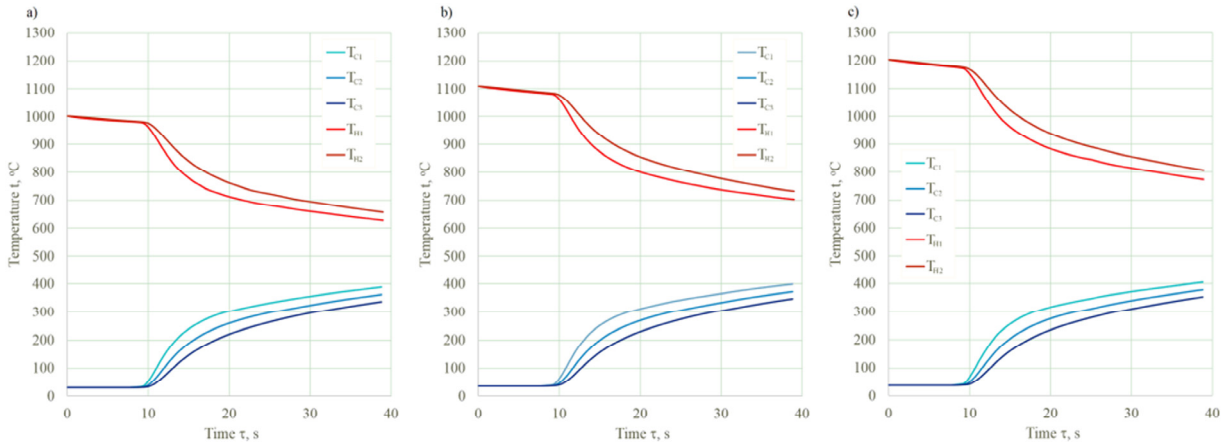

Fig. 3. The temperature distribution vs. time for the initial sample temperature obtained in the experiment: a) 1000°C – test 1000, b) 1100°C – test 1100, c) 1200°C – test 1200

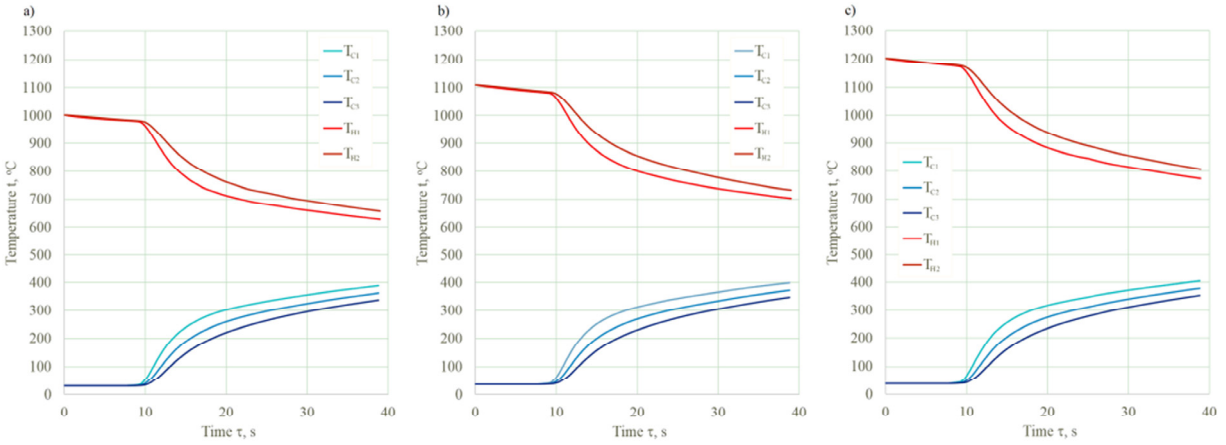

Fig. 4. The heat flux as a function of time for the initial temperature; a) test 1000, b) test 1100, c) test 1200

made separately for the Cold and Hot samples. The average deviation of the computed temperatures from the measured ones for all cases is lower than 3°C. The heat flux depends on the Hot sample temperature, when it increases, so does the value of heat flux transferred between the sample faces. There is a small difference between the curves obtained from the inverse solution for the Cold and Hot samples (Fig. 4), which confirms that the determined heat flux value is correct.

3. Verification of calculation results

The obtained solution was verified with the Ansys Fluent package. To this end a geometric model of samples used in the experiment was built and a finite element mesh was constructed. 3D models were applied for both samples, taking into account the insulation for the Hot sample. To minimise the mesh and to shorten the computing time for the Hot sample, its symmetry was used and the computation was performed for 1/2 of its volume. The mesh for this sample comprised 227 632 elements, whereas for the Cold sample it was 186 907 elements. The boundary conditions on all faces were implemented with the user-defined function (UDF). The change in the value of the heat flux at the contact face as a function of time was approximated with a polynomial in the form of:

$$q_s(\tau) = a_3\tau^3 + a_2\tau^2 + a_1\tau + a_0 \tag{2}$$

where: q_s – heat flux at the contact face, W/m^2; a_i – polynomial coefficients (values are presented in Table 2), -; t – time, s

The boundary conditions at the sample side faces were the same as in the inverse calculation and were applied in the following form:

$$\dot{q_{sf}} = h_{sf}(t_{sf} - t_a) \tag{3}$$

where: h_{sf} – the heat transfer coefficient at the side face, W/m^{2}K; t_{sf} – the side face temperature of the Hot or Cold sample, °C; t_a – ambient temperature, °C.

At the bottom face of each sample, the heat flux was defined:

$$\dot{q_b} = h_b(t_b - t_a) \tag{4}$$

where: h_b – the heat transfer coefficient at the bottom face, W/m^{2}K; t_b – the bottom face temperature of the Hot or Cold sample, °C.

The boundary conditions at the side faces had a strong influence on the accuracy of the inverse solution. To complete

TABLE 2

Third degree polynomial coefficients (2)

Time interval s	Sample	Function
Test 1000		
0.0 7.5	Cold	—
	Hot	$1.0668E{+}02\tau^3 - 4.6631E{+}02\tau^2 - 1.1173E{+}04\tau + 1.0426E{+}05$
7.5 8.9	Cold	$-7.7881E{+}03\tau^3 + 1.9511E{+}05\tau^2 - 1.6042E{+}06\tau + 4.3666E{+}06$
	Hot	$6.4128E{+}03\tau^3 - 1.4280E{+}05\tau^2 + 1.0597E{+}06\tau - 2.5818E{+}06$
8.9 9.2	Cold	$-2.5959E{+}06\tau^3 + 7.1931E{+}07\tau^2 - 6.6350E{+}08\tau + 2.0376E{+}09$
	Hot	$-3.1892E{+}06\tau^3 + 8.7880E{+}07\tau^2 - 8.0637E{+}08\tau + 2.4641E{+}09$
9.2 11.0	Cold	$-7.7881E{+}03\tau^3 + 1.9511E{+}05\tau^2 - 1.6042E{+}06\tau + 4.3666E{+}06$
	Hot	$-3.6175E{+}04\tau^3 + 9.1838E{+}05\tau^2 - 6.8800E{+}06\tau + 1.3963E{+}07$
11.0 13.5	Cold	$1.6113E{+}04\tau^3 - 6.5450E{+}05\tau^2 + 8.7781E{+}06\tau - 3.7546E{+}07$
	Hot	$1.1162E{+}04\tau^3 - 4.6986E{+}05\tau^2 + 6.4912E{+}06\tau - 2.8145E{+}07$
13.5 20.0	Cold	$-8.5269E{+}01\tau^3 + 7.3945E{+}03\tau^2 - 2.3857E{+}05\tau + 3.4020E{+}06$
	Hot	$-6.4948E{+}00\tau^3 + 4.1259E{+}03\tau^2 - 1.9937E{+}05\tau + 3.2700E{+}06$
20.0 39.0	Cold	$-4.2572E{+}01\tau^3 + 4.4801E{+}03\tau^2 - 1.6947E{+}05\tau + 2.8431E{+}06$
	Hot	$-3.6749E{+}01\tau^3 + 3.9478E{+}03\tau^2 - 1.5243E{+}05\tau + 2.6435E{+}06$
Test 1100		
0.0 7.5	Cold	—
	Hot	$2.0399E{+}02\tau^3 - 1.7846E{+}03\tau^2 - 5.9977E{+}03\tau + 1.1621E{+}05$
7.5 8.9	Cold	$4.0050E{+}04\tau^3 - 9.9819E{+}05\tau^2 + 8.3083E{+}06\tau - 2.3039E{+}07$
	Hot	$-1.9483E{+}03\tau^3 + 4.8349E{+}04\tau^2 - 3.9468E{+}05\tau + 1.1194E{+}06$
8.9 9.2	Cold	$-7.0609E{+}06\tau^3 + 1.9299E{+}08\tau^2 - 1.7573E{+}09\tau + 5.3310E{+}09$
	Hot	$-8.6492E{+}06\tau^3 + 2.3613E{+}08\tau^2 - 2.1478E{+}09\tau + 6.5090E{+}09$
9.2 11.0	Cold	$-1.8223E{+}04\tau^3 + 3.8229E{+}05\tau^2 - 1.5648E{+}06\tau - 3.4708E{+}06$
	Hot	$-4.7110E{+}04\tau^3 + 1.2569E{+}06\tau^2 - 1.0363E{+}07\tau + 2.5941E{+}07$
11.0 13.0	Cold	$9.6229E{+}03\tau^3 - 4.3449E{+}05\tau^2 + 6.3018E{+}06\tau - 2.8236E{+}07$
	Hot	$5.5235E{+}03\tau^3 - 2.7934E{+}05\tau^2 + 4.3405E{+}06\tau - 1.9973E{+}07$
13.0 20.0	Cold	$-1.6379E{+}02\tau^3 + 1.2370E{+}04\tau^2 - 3.4081E{+}05\tau + 4.0935E{+}06$
	Hot	$-1.7245E{+}02\tau^3 + 1.3285E{+}04\tau^2 - 3.6580E{+}05\tau + 4.2636E{+}06$
25.0 39.0	Cold	$-3.4039E{+}01\tau^3 + 3.6516E{+}03\tau^2 - 1.4288E{+}05\tau + 2.5699E{+}06$
	Hot	$2.3689E{+}00\tau^3 + 1.1237E{+}02\tau^2 - 2.9814E{+}04\tau + 1.3688E{+}06$
Test 1200		
0.0 7.5	Cold	—
	Hot	$2.0766E{+}02\tau^3 - 1.7415E{+}03\tau^2 - 7.1115E{+}03\tau + 1.1861E{+}05$
7.5 8.9	Cold	$5.6526E{+}04\tau^3 - 1.4154E{+}06\tau^2 + 1.1838E{+}07\tau - 3.2997E{+}07$
	Hot	$3.1023E{+}03\tau^3 - 5.5310E{+}04\tau^2 + 3.0801E{+}05\tau - 4.5267E{+}05$
8.9 9.2	Cold	$-8.4405E{+}05\tau^3 + 2.4743E{+}07\tau^2 - 2.3978E{+}08\tau + 7.6926E{+}08$
	Hot	$-1.1535E{+}07\tau^3 + 3.1423E{+}08\tau^2 - 2.8521E{+}09\tau + 8.6257E{+}09$
9.2 11.0	Cold	$8.4966E{+}04\tau^3 - 2.8292E{+}06\tau^2 + 3.1650E{+}07\tau - 1.1759E{+}08$
	Hot	$-3.2831E{+}04\tau^3 + 8.6276E{+}05\tau^2 - 6.8352E{+}06\tau + 1.5787E{+}07$
11.0 13.5	Cold	$7.1778E{+}03\tau^3 - 3.4551E{+}05\tau^2 + 5.2353E{+}06\tau - 2.4016E{+}07$
	Hot	$1.0896E{+}03\tau^3 - 1.2875E{+}05\tau^2 + 2.6737E{+}06\tau - 1.3985E{+}07$
13.5 20.0	Cold	$-1.3833E{+}02\tau^3 + 1.1055E{+}04\tau^2 - 3.2093E{+}05\tau + 4.0257E{+}06$
	Hot	$-5.0280E{+}02\tau^3 + 2.9397E{+}04\tau^2 - 6.2228E{+}05\tau + 5.6313E{+}06$
20.0 39.0	Cold	$-3.8295E{+}01\tau^3 + 4.1110E{+}03\tau^2 - 1.5919E{+}05\tau + 2.7681E{+}06$
	Hot	$-3.8196E{+}01\tau^3 + 4.2200E{+}03\tau^2 - 1.6693E{+}05\tau + 2.8774E{+}06$

the boundary conditions, the heat transfer coefficients h_{sf}, h_b were specified. The boundary conditions at the side faces of the samples take into account heat loss due to radiation and convection:

$$h_{sf} = h_{rad} + h_{con} \tag{5}$$

where:

$$h_{con} = \frac{Nu * \lambda}{z} \tag{6}$$

For the Hot sample the following dependencies were used in the calculations [13,14]:

$$h_{rad} = \left(0.93 - 48.8E - 5 * T_{ss}\right) * 5.675 * 10^{-8} \frac{T_{ss}^4 - T_a^4}{T_{ss} - T_a} \quad (7)$$

where: $T_{ss} = t_{ss} + 273$; $T_a = t_a + 273$ and

$$h_b = 300 \text{ W/m}^2\text{K} \quad (8)$$

For the Cold sample the following dependencies were used in the calculations [13]:

$$h_{rad} = \left(1.2 - 0.52\frac{T_{ss}}{1000}\right) * 5.675 * 10^{-8} \frac{T_{ss}^4 - T_a^4}{T_{ss} - T_a} \quad (9)$$

and

$$h_b = 300 * \left(1 + \frac{\tau}{30}\right) \quad (10)$$

where: τ – time, s.

The sample material properties, necessary to solve the problem, were expressed as functions of temperature [15].

Table 3 presents the average absolute error of temperature field computing with the Ansys Fluent package, compared to the measurement results, determined for points corresponding to the location of thermocouples at the test stand. The average absolute error was defined:

$$\delta t = \frac{1}{k}\sum_{i=1}^{k}\left(\frac{\sum_{j=1}^{n}\sqrt{\left(t_{i,j}^{mea} - t_{i,j}^{cal}\right)^2}}{n}\right) \quad (11)$$

where: k – number of sensors, for Cold samples $k = 3$, for Hot samples $k = 2$; n – number of time steps; $t_{i,j}^{mea}$ – the sample temperature measured by the sensor i at the time τ_j; $t_{i,j}^{cal}$ – the sample temperature at the location of the sensor i at the time τ_j calculated from the Ansys Fluent package.

The maximum value of the average error is less than 3°C, which confirms that the boundary condition for the contact surface was determined correctly with the described test method.

TABLE 3

Average absolute error of temperature determination

Test name	Sample	Average absolute error of temperature determination δt [°C]
1000	Cold	1.36
	Hot	1.79
1100	Cold	1.57
	Hot	2.92
1200	Cold	1.46
	Hot	3.76

5. Analysis of accuracy of determining the heat flux with fractional design

The output parameter, or heat flux, identified on the basis of the inverse solution, is determined indirectly. Errors of all physical parameters occurring in the model influence the accuracy of determining the parameter concerned. The value of each input parameter is encumbered with its determination error, resulting from the method applied to determine a specific parameter. These errors affect the accuracy and equivalence of the inverse problem solution for the heat conduction equation. The fractional design method [16,17] was used in the examinations, and the impact of the following input parameters was analysed:

– thermal conductivity λ,
– specific heat c_p,
– accuracy of determining the boundary conditions at the side h_{ss} and bottom h_b faces.

It was assumed that the maximum error made at estimating these input parameters was ±10%. The number of factors considered was 4, so the number of tests was $2^4 = 16$. All possible combinations are presented in Table 4. The parameters tested were labelled with letters: A, B, C, D.

TABLE 4

The matrix of the experiment

Test number	λ	c_p	h_{ss}	h_b	Label
	A	B	C	D	
1.	–10%	–10%	–10%	–10%	(1)
2.	+10%	–10%	–10%	–10%	a
3.	–10%	+10%	–10%	–10%	b
4.	+10%	+10%	–10%	–10%	ab
5.	–10%	–10%	+10%	–10%	c
6.	+10%	–10%	+10%	–10%	ac
7.	–10%	+10%	+10%	–10%	bc
8.	+10%	+10%	+10%	–10%	abc
9.	–10%	–10%	–10%	+10%	d
10.	+10%	–10%	–10%	+10%	ad
11.	–10%	+10%	–10%	+10%	bd
12.	+10%	+10%	–10%	+10%	abd
13.	–10%	–10%	+10%	+10%	cd
14.	+10%	–10%	+10%	+10%	acd
15.	–10%	+10%	+10%	+10%	bcd
16.	+10%	+10%	+10%	+10%	abcd

Average relative computing errors determined for three computing variants and both samples are presented in the graph (Fig. 5). For all tests performed, the error value ranges from 4.61% to 10.94% for computing performed for the Cold sample, and from 5.16% to 12.21% for the Hot sample. An analysis of assessment of the impact of individual parameters on the value of total error allows us to find that parameters A and B affect the final result the most; these are the thermal conductivity and specific heat (Fig. 6). For the presented calculations, the contribution of the specific heat error to the total error ranges from 82.90% to 87.33%. The heat transfer coefficient, ranked second in terms of impact, contributes from 12.08% to 16.61%. The contribution of the inaccuracy of determining heat transfer through the other sample faces – the side and bottom ones – is the lowest. Their impact is between 0.11% and 0.41% for the side face, and between 0.01% and 0.21% for the bottom face. Effects of all other impacts are negligible.

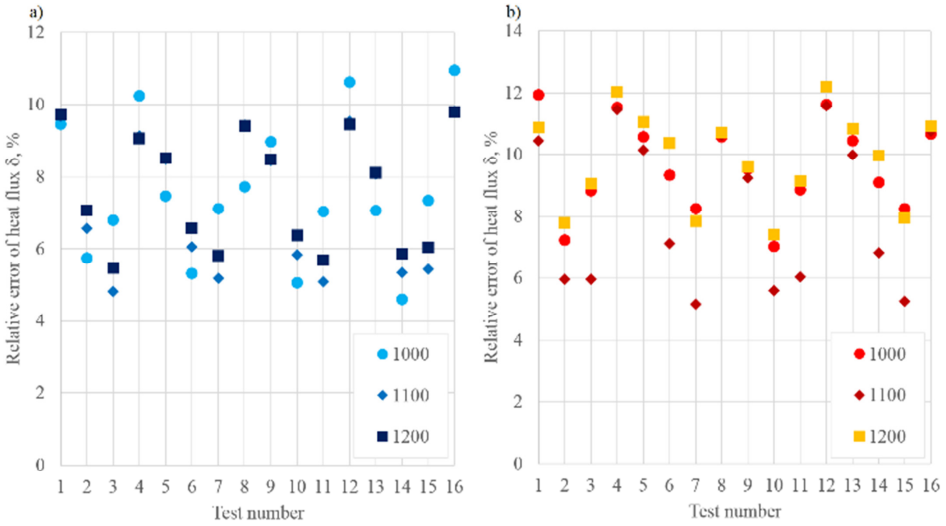

Fig. 5. The average relative errors of the calculation of the heat flux for the test selected for the fractional design method

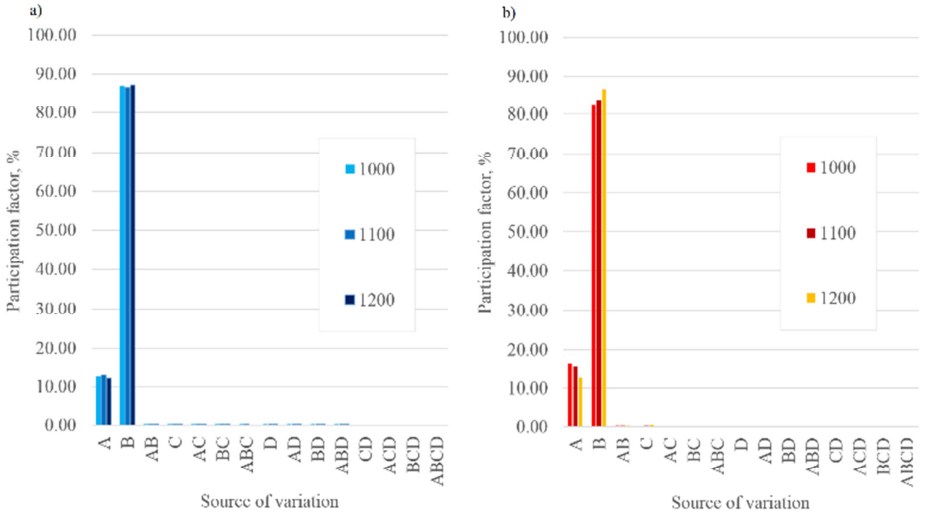

Fig. 6. Participation of the factor error in the total error of inverse calculation of heat flux for all sources of variation

4. Heat transfer in the continuous steel casting process

The obtained distribution of heat flux versus the experiment time is only correct for the system analysed, and the solid sizes used in the experiment. Therefore it must not be generalised onto other cases. The results of computing with the described methodology can be presented in a more useful manner, as a function of a parameter not directly related to the nature of the experiment. This parameter can be the surface temperature of the solid, for which it will be applied in the numerical computation to model the heat transfer in industrial processes.

Using the results of computation, the distribution of changes in heat flux versus the surface temperature for the contact of rolls with the strand surface in the continuous casting machine was determined. The changes in the heat transfer coefficient value were approximated with a polynomial in the form:

$$h_s\left(t_s\right) = a_4 {t_s}^4 + a_3 {t_s}^3 + a_2 {t_s}^2 + a_1 t_s + a_0 \qquad (12)$$

where: h_s – heat transfer coefficient at the contact face, W/m^{2}K; a_i – polynomial coefficients (values are presented in Table 5), -; t_s – surface temperature, s.

TABLE 5

Third degree polynomial coefficients (12)

Test	Function	Temperature range	Average relative error
1000	$-3.2102\text{E}{-}03 t_s^3 - 2.3164\text{E}{+}01 t_s^2 + 4.2766\text{E}{+}04 t_s - 1.6354\text{E}{+}07$	950-650	0.58%
1100	$-3.2847\text{E}{-}02 t_s^3 + 5.9999\text{E}{+}01 t_s^2 - 2.8384\text{E}{+}04 t_s + 2.3211\text{E}{+}06$	1060-725	0.47%
1200	$-3.2847\text{E}{-}02 t_s^3 + 5.9999\text{E}{+}01 t_s^2 - 2.8384\text{E}{+}04 t_s + 2.3211\text{E}{+}06$	1130-800	0.58%

The presented method of heat transfer description at the contact of two bodies at high temperatures was used for the numerical modelling of the steel continuous casting process. The

original numerical package PM-COS, developed by employees of the Department of Thermal Engineering and the Environment Protection, allows the solidifying strand temperature field to be computed. The description of the model and the algorithm can be found in papers written by the authors of the computer program [2,15]. In the computing, the formulas describing the value of the heat transfer coefficient versus the surface temperature presented in Table 5 were implemented to the boundary conditions module.

The computation was performed for steel C45, which was used in the experimental research, and a 225 × 1500 mm strand cast at a rate of 0.6 m/min. The roll position was assumed in a layout typical for this type of equipment [4], and the pressure force value was selected on the basis of literature data [18]. The numerical computation of the strand cooling process was performed for variants without (Test 1) and with rolls (Test 2).

The graph (Fig. 7) presenting the change in the surface temperature allows us to assess the impact of heat transfer through the contact of the strand surface with the rolls on the surface temperature of the solidifying CC strand. Differences in the temperature changes occurring along the strand length are rather significant. In the places where the strand surface touches the rolls the temperature rapidly drops, and this temperature drop is later compensated by heat conduction to the strand surface from its inside.

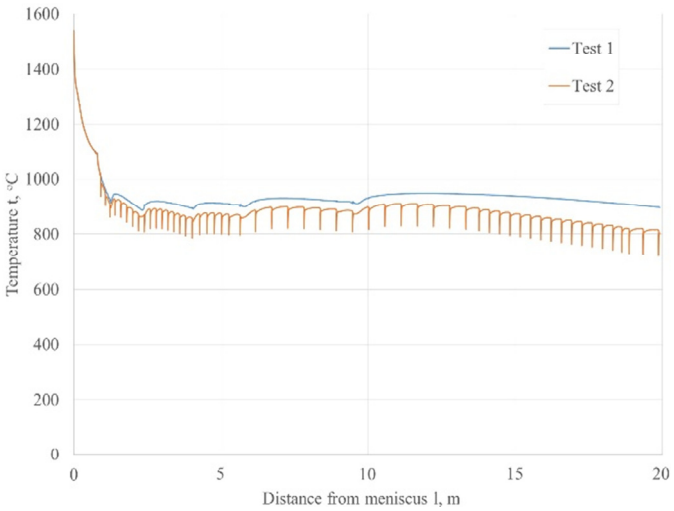

Fig. 7 Changes in the CC strand top face temperature

5. Conclusion

The paper presents a model of heat transfer between two solid faces being in contact as a result of the force applied. The value of heat flux was obtained from original research using a new methodology for its determination. It consists of two stages: experiment and numerical computations. The impact of the measurement error of the parameters set in the inverse solution on the computation result was analysed. The parameters were: heat transfer coefficient, specific heat, and boundary conditions at the side and bottom faces. Test calculations, in which measurement errors of these parameters were simulated and their influence on the accuracy of the obtained solution was analysed, were conducted. The conducted tests of the solution uniqueness confirmed that a high accuracy model of heat transfer in the described system was obtained.

In the final part of the study, the possibility of application of the developed boundary conditions in the form of heat flux determined in numerical computations for industrial processes was illustrated by the determination of the distribution and changes of the temperature field in the process of steel continuous casting. The contact of the strand surface with withdrawal and support rolls was taken into account.

The prevailing method of heat transfer in the secondary zone is water spray cooling, with a share of ca. 90%. The complimentary heat transfer mechanism is the contact with support and withdrawal rolls. Neglecting this method of heat discharge may lead to obtaining incorrect results of numerical calculations of the temperature field in the solidifying strand, in particular at the strand surface. The complete description of cooling within the steel continuous casting process is complemented by the heat transfer as a result of strand cooling in the air.

Acknowledgments

The study was performed as part of regular activity, AGH University of Science and Technology, Faculty of Metals Engineering and Industrial Computer Science.

REFERENCES

[1] A. Cwudziński, J. Jowsa, P. Przegrałek, Archives of Metallurgy and Materials **61**(4), 2013-2020 (2016).

[2] M. Rywotycki, Z. Malinowski, J. Giełżecki, A. Gołdasz, Archives of Metallurgy and Materials **59** (2), 487-492 (2014).

[3] W. Oberaigner, R. Leitner, Innovation highlights in continuous casting automation. VII Międzynarodowa konferencja COS, Krynica (2016).

[4] Y. Meng, B.G. Thomas, Metallurgical and Materials Transactions B **34B**, 685-705 (2003)

[5] J. S. Ha, J. R. Cho, B. Y. Lee, M.Y. Ha, Journal of Materials Processing Technology **113**, 257-261 (2001).

[6] J. Falkus (ed.), Modelowanie procesu ciągłego odlewania stali. Wydawnictwo Naukowe Instytutu Technologii Eksploatacji – Państwowy Instytut Badawczy, Radom 2012.

[7] M. Krzyżanowski, J.H. Beynon, Materials Science and Technology **32**, 407-417 (2016).

[8] M. Rywotycki, Z. Malinowski, A. Szajding, J. Falkus, K. Sołek, K. Miłkowska-Piszczek, Hutnik Wiadomości Hutnicze **83**, 13-17 (2016).

[9] R. Wyczółkowski, T. Wyleciał, Hutnik-WH **84** (5), 225-228 (2017).

[10] Y. Zhao, D.F. Chen, M.J. Long, J.L. Shen, R.S. Qin, Ironmaking and Steelmaking **415**, 377-386 (2014).

[11] B. Barber, B. Patrick, H. Sha, K.H. Spitzer, R. York, R. Scholz, R. Jeschar, H. Kraushaar, Determination of strand surface temperatures in continuous casting. European Commission Technical Steel Research Steelmaking, Luxembourg (1998).
[12] M. Rywotycki, Archives of Metallurgy and Materials **61** (4), 2061-2070 (2016).
[13] Z. Malinowski, J.G. Lenard, M.E. Davies, Journal of Materials Processing Technology **41** (2), 125-142 (1994).
[14] P. Mullinger, B. Jenkins, Industrial and process furnaces: principles, design and operation, Elsevier, Butterworth,-Heineman, (2008).
[15] M. Rywotycki, Wymiana ciepła w warunkach kontaktu narzędzia i materiału w wysokotemperaturowych procesach metalurgicznych, Wydawnictwa AGH, Kraków (2017).
[16] W. Volk, Statystyka dla inżynierów, Wydawnictwa Naukowe – Techniczne, Warszawa (1973).
[17] A. Cebo, Archives of Metallurgy and Materials **55** (2), 429-434 (2010).
[18] N.V. Rachchh, R. K. Misra, International Journal of Management, IT and Engineering **2**, 82-102 (2012).